# Investigation on Masticatory Muscular Functionality Following Oral Reconstruction – An Inverse Identification Approach

Keke Zheng[a,#], Zhipeng Liao[a,#], Nobuhiro Yoda[b], Jianguang Fang[c], Junning Chen[d], Zhongpu Zhang[a], Jingxiao Zhong[a], Christopher Peck[e], Keiichi Sasaki[b], Michael V Swain[a], Qing Li[a,*]

[a]School of Aerospace, Mechanical and Mechatronic Engineering, The University of Sydney, NSW 2006, Australia

[b]Division of Advanced Prosthetic Dentistry, Tohoku University Graduate School of Dentistry, 4-1 Seiryo-machi, Aoba-ku, Sendai, Japan 9808575

[c]School of Civil and Environmental Engineering, University of Technology Sydney, NSW 2006, Australia

[d]College of Engineering, Mathematics, and Physical Sciences, University of Exeter, EX4 4QF United Kingdom

[e]Faculty of Dentistry, The University of Sydney, NSW 2006, Australia

[*]Correspondence to: Qing Li

[#]: These authors contributed equally to this study

Room S542, Mechanical Engineering Building (J07),

Darlington Campus, The University of Sydney, NSW 2006, Australia

Phone: +61-02 9351 8607; Fax: +61-02 9351 7060;

Email: qing.li@sydney.edu.au

Word count: 3495

**Abstract**

The human masticatory system has received significant attention in the areas of biomechanics due to its sophisticated co-activation of a group of masticatory muscles which contribute to the fundamental oral functions. However, determination of each muscular force remains fairly challenging *in vivo*; the conventional data available may be inapplicable to patients who experience major oral interventions such as maxillofacial reconstruction, in which the resultant unsymmetrical anatomical structure invokes a more complex stomatognathic functioning system. Therefore, this study aimed to (1) establish an inverse identification procedure by incorporating the sequential Kriging optimization (SKO) algorithm, coupled with the patient-specific finite element analysis (FEA) *in silico* and occlusal force measurements at different time points over a course of rehabilitation *in vivo*; and (2) to evaluate muscular functionality for a patient with mandibular reconstruction using a fibula free flap (FFF) procedure. The results from this study proved the hypothesis that the proposed method is of certain statistical advantage of utilizing occlusal force measurements, compared to the traditionally adopted optimality criteria approaches that are basically driven by minimizing the energy consumption of muscle systems engaged. Therefore, it is speculated that mastication may not be optimally controlled, in particular for maxillofacially reconstructed patients. For the abnormal muscular system in the patient with orofacial reconstruction, the study shows that in general, the magnitude of muscle forces fluctuates over the 28-month rehabilitation period regardless of the decreasing trend of the maximum muscular capacity, which implies that the reduction of the masticatory muscle activities on the resection side might lead to non-physiological oral biomechanical responses, which can change the muscular activities for stabilizing the reconstructed mandible.

**Keywords**: Muscle forces, Occlusal force, Mandibular reconstruction, Inverse identification, Sequential Kriging Optimization (SKO), Optimality criteria.

## 1. Introduction

Human masticatory functionality and capability is consummated by co-energizing a bunch of masticatory muscles that contribute to the execution of chewing, biting, clenching, proper speech, jaw movement, etc, in a highly sophisticated manner. The form of mastication and thus stomatognathic performance would be substantially perturbed, and in most likelihood deteriorate, following major oral interventions, such as the instalment of dental prosthesis and maxillofacial reconstruction (Marunick et al., 1992a; Pepato et al., 2013; RENAUD et al., 1984). While the influence of muscular alteration on masticatory efficiency induced by different oral surgeries has been explored in literature, the observations remain rather inconsistent and even controversial among those studies (Endo, 1972; Namaki et al., 2004). Despite the fact that such conflicts may be ascribable to various factors, such as the demographic variance of the subjects and different nature of cranio-maxillo-facial surgeries, lack of an effective and accurate measurement technique makes solution of this issue rather challenging. Therefore, a new measurement system or protocol for determination of mastication *in vivo*, normally functioning or even potentially malfunctioning, is required.

Over decades, various techniques have been developed to qualitatively or quantitatively determine muscular activities, such as electromyography (EMG) (Fukunaga et al., 2001; Van Ruijven and Weijs, 1990), computed tomography (CT) (Katsumata et al., 2004) and optimization methods (Schindler et al., 2007). Each technique has its own advantages yet considerable limitations. For example, EMG is *in vivo* in nature but known for its incapability to accurately quantify joint reactions and characteristics of motor skills, including the exact force magnitude, orientation and muscle force ratio (Hattori et al., 2003). The CT technique is only able to approximate the maximum capacity of muscular magnitude and its direction (Katsumata et al., 2004). The optimization methods allow accommodating static equilibrium and physiological constraints for estimating the magnitude, orientation and activation ratio (AR) of muscular functional groups in various movements (Chou et al., 2015; Schindler et al., 2007), by minimizing the summed muscle forces (Pedotti et al., 1978), summed joint forces (Osborn and Baragar, 1985), summed reaction forces or summed elastic energies (Schindler et al., 2007), but it remains uncertain which or any of these optimality criteria is correct most universally, with conflicting results recorded. The criteria of minimal energy (Rues et al., 2008; Schindler et al., 2007), minimal activation ratio (Pedotti et al., 1978) and combination of minimal muscle force and moment (Seireg and Arvikar, 1973) were respectively found to better agree with the EMG data for various groups of subjects in comparison with the other criteria. However, there is lack of solid evidence and consensus about which, if any, of such optimality criteria, can be applied to characterize muscle forces, in particular to the patients undertaking major oral interventions.

This study thus aimed to (1) propose a physiologically validated and clinically applicable approach for the quantification of muscular activity through a mandibulectomy follow-up; (2) compare the established inverse identification approach with the existing optimality criteria through statistical models; and (3) analyze the muscular behaviour following the mandibular resection at different rehabilitation stages.

## 2. Materials and Methods

### 2.1 Clinical treatment and medical imaging analysis

A male patient aged 66, diagnosed with the squamous-cell carcinoma at the right molar gingiva in August 2013, was recruited to undergo the mandibular reconstruction with osteotomized fibular free flap (FFF). The fibular bone was harvested, segmented and modeled to accommodate the defect morphology, followed by the installation of a titanium reconstruction plate (Synthes, Solothurn, Switzerland) which was configured to be fixed monocortically. The CT scans were performed before the surgery and at 4, 16 and 28 months after the surgery, denoted as BS (before surgery), M4, M16 and M28, respectively.

The occlusal forces on the remaining teeth were measured after surgery at M4, M16 and M28 with a pressure-indicating film (Dental Prescale 50H, type R, Fuji Photo Film Co., Tokyo, Japan) (Hidaka et al., 1999) (Fig. 1a) as the study aimed to quantify the muscle force after the mandibular reconstruction. The force magnitudes were calculated by scanning the films using a pre-calibrated device (Occluzer FPD 707, Fuji Photo Film Co.). Bite records were acquired using silicone impression (Flexicon, injection type, GC Co., Tokyo, Japan) to identify coloured spots on the film and hence determine the occlusal contact regions on the lower arches (Fig. 1b & c).

The maximum muscle force ($F_{max}$), or the maximum muscular capacity (MMC) was determined by multiplying the muscle's physiological cross-sectional area ($PCSA$) with a constant of $\lambda = 4 \times 10^{-3}$ N/cm$^2$ (Hattori et al., 2003; Peck et al., 2000; Pruim et al., 1980; Weijs and Hillen, 1985). Thus, each muscle force was determined according to the following formula:

$$F_{max} = PCSA \times \lambda \quad (1)$$

The $PCSA$ was obtained from whole muscle cross-sections measured from the CT sectional images of this patient (Fig. 2). The measurement was conducted according to the existing techniques established (Weijs and Hillen, 1984, 1985). The $PCSA$ of each muscle, included the left masseter (MA), left medial pterygoid (MP), left temporalis (T) muscle, left lateral pterygoid (LLP) and right lateral pterygoid (RLP) muscle, was estimated by selecting the largest one from the reference plane as well as the 10 planes that lie from 1 to 5 mm above and below or anterior and posterior of each reference plane (Fig. 2).

## 2.2 Finite element modeling

CT images at BS, M4, M16 and M28 were registered and segmented with ScanIP 7.0 (Simpleware Ltd, Exeter, UK) and Amira 4.1.2 (Mercury Computer Systems, Inc., Chelmsford, MA, USA); based upon which the parametric non-uniform rational basis splines (NURBs) models were generated using Rhinoceros (Robert McNeel & Associates, Seattle, US); and imported into finite element (FE) analysis code ABAQUS 6.11 (Dassault Systèmes, Tokyo, Japan). The bony tissues were featured with the CT-based heterogeneous distribution (Field et al., 2010), which were calculated through interpolation between the lowest and highest densities in terms of Hounsfield units (*HU*) (Liao et al., 2016). The orthotropic cortical layer was also incorporated by employing the curve fitting results as presented in (Liao et al., 2017). The full details of FE modeling, including the material properties, loading and boundary conditions, as shown in Fig. 3, were established by following our previous studies (Chen et al., 2015; Liao et al., 2015). The scalar components that form the vector of each resultant muscle force are summarized in Table 1.

**Table 1** Details of scalar components of the vector representing each resultant muscle force (Unit: N)

| | $\mathbf{F}_{\mathbf{Ma}}$ | | | $\mathbf{F}_{\mathbf{MP}}$ | | | $\mathbf{T}$ | | |
|---|---|---|---|---|---|---|---|---|---|
| | $MA_x$ | $MA_y$ | $MA_z$ | $MP_x$ | $MP_y$ | $MP_z$ | $T_x$ | $T_y$ | $T_z$ |
| **M4** | 5.46 | 1.16 | 116.86 | -25.66 | 8.88 | 112.63 | 41.69 | -15.96 | 99.15 |
| **M16** | 3.51 | 1.2 | 114.48 | -22.89 | 14.57 | 63.54 | 11.05 | -30.31 | 111.83 |
| **M28** | 2.15 | 0.9 | 103.8 | -50.37 | 18.61 | 89.25 | 17.42 | -29.31 | 113.69 |
| | $\mathbf{F}_{\mathrm{LLP}}$ | | | $\mathbf{F}_{\mathrm{RLP}}$ | | | | | |
| | $LPL_x$ | $LPL_y$ | $LPL_z$ | $LPR_x$ | $LPR_y$ | $LPR_z$ | | | |
| **M4** | -30.41 | 79.8 | -12.63 | 37.94 | 89.88 | -7.26 | | | |
| **M16** | -24.29 | 23.54 | -3.61 | 24.31 | 23.54 | -3.61 | | | |
| **M28** | -44.11 | 27.03 | -9.96 | 42.6 | 36.66 | -3.69 | | | |

## 2.3 Inverse identification of muscle forces

Inverse identification can be defined to minimize the deviation between the experimental measurement and numerical prediction in terms of unknown muscle force components ($\mathbf{x}$), as:

$$\begin{cases} \min \quad -J(\mathbf{x}) = -J(\mathbf{F}_{\mathrm{Ma}}, \mathbf{F}_{\mathrm{MP}}, \mathbf{T}, \mathbf{F}_{\mathrm{LLP}}, \mathbf{F}_{\mathrm{RLP}}) \\ \mathrm{s.t.} \quad [1.56, 0.83, 1.72, 0.53, 1.15, 0.99]^{\mathrm{T}} \le \left[\frac{M_a}{MP}, \frac{M_a}{T}, \frac{M_a}{LP}, \frac{MP}{T}, \frac{MP}{LP}, \frac{T}{LP}\right]^{\mathrm{T}} \le [2.15, 2.15, 4.07, 1.16, 2.61, 4.92]^{\mathrm{T}} \\ \qquad [59\ \mathrm{N}, 39\ \mathrm{N}, 34\ \mathrm{N}, 34\ \mathrm{N}]^{\mathrm{T}} \le [M_a, MP, T, LP]^{\mathrm{T}} \le [372\ \mathrm{N}, 264\ \mathrm{N}, 279\ \mathrm{N}, 382\ \mathrm{N}]^{\mathrm{T}} \end{cases} \tag{2}$$

where $\mathbf{F}_{\mathrm{Ma}}, \mathbf{F}_{\mathrm{MP}}, \mathbf{T}, \mathbf{F}_{\mathrm{LLP}}, \mathbf{F}_{\mathrm{RLP}}$ are defined as the muscle force vectors for Ma, MP, T, LLP and RLP (Table 1), respectively. The physiological constraints, which are based upon a series of previous literature studies (Al-Ahmari et al., 2015; Cruz et al., 2003; Faulkner et al., 1987; Gonda et al., 2014; Korioth et al., 1992; Osborn and Baragar, 1985) and the CT measurements obtained from this study, were utilized for establishing the minimum and maximum magnitudes; and the muscle group ratios that restrict the relative magnitudes among different groups of muscles.

The cost function in terms of the deviation, $J(\mathbf{x})$, can be formulated as:

$$J(\mathbf{x}) = 1 - \frac{\sum_{i=1}^{N}\left(F_{Oi} - F_{Ri}(\mathbf{x})\right)^2}{\sum_{i=1}^{N}(F_{Oi} - \bar{F}_O)^2} \tag{3}$$

where $i$ denotes the number of reaction forces (or occlusal measurements), $N$ is the number of muscle force components ($N = 12$ here). $F_{Oi}$ and $F_{Ri}$ are the experimental measurements of occlusal forces and the resultant reaction forces obtained from the FE prediction, as

$$F_{Ri} = |\mathbf{F}_{Ri}| \tag{4}$$

where $\mathbf{F}_{Ri}$ represents the vector of FE occlusal reactions on the mandibular canine (C), first premolar ($P_1$), second premolar ($P_2$) and second molar ($M_2$), respectively. $\bar{F}_O$ is the average measurements of occlusal loads used to normalize the deviation of the cost function (Eq. (3)).

To reduce the computational cost due to iterative analysis, surrogate modeling techniques are commonly employed as an alternative for formulating the responses of interest as per a simple and explicit function with unknowns to be determined, such as the components of muscle forces in this particular case. In the application of surrogate-based optimization, the Sequential Kriging Optimization (SKO) algorithm, which considers both local region exploitation and global exploration in whole design space, was adopted here to determine the unknown muscle force components by matching the numerical simulation results with the clinical measurement data. The detail of this method can be referred to a previous study (Fang et al., 2017).

To compare the proposed SKO approach with conventional gradient-based optimization for its effectiveness and reliability in determining muscle forces, four commonly used gradient-based optimizations driven by energy-consumption-minimizing strategy were also considered here. Of them, several aforementioned optimization criteria, such as minimization of the summed muscle forces ($F_M$), minimization of summed joint forces ($F_J$), minimization of summed reaction forces ($F_R$) and minimization of summed elastic energies were defined as in Eqs. (5)-(8), respectively (Pedotti et al., 1978, Osborn and Baragar, 1985, Schindler et al., 2007):

$$\min f_1 = \sum F_M \tag{5}$$

$$\min f_2 = \sum F_J \tag{6}$$

$$\min f_3 = \sum F_R \tag{7}$$

$$\min f_4 = \sum \left( \frac{l_F}{\mathrm{A}\cos^2 \alpha} F_M^2 \right) \tag{8}$$

where $l_F$, A and $\alpha$ represents fibre length, physiological cross-section and pennation angle, respectively.

The constraints of each optimization problem were defined to be the muscle forces, occlusal and TMJ loads which should satisfy the static equilibrium of forces and moments, as follows:

$$\sum \mathbf{F} = \sum \mathbf{F}_m + \sum \mathbf{F}_j + \sum \mathbf{F}_R = \mathbf{0} \tag{9}$$

$$\sum \mathbf{M} = \sum \mathbf{r}_m \times \mathbf{F}_m + \sum \mathbf{r}_j \times \mathbf{F}_j + \sum \mathbf{r}_R \times \mathbf{F}_R = \mathbf{0} \tag{10}$$

where $\mathbf{F}_m$, $\mathbf{F}_j$ and $\mathbf{F}_R$ are muscular, joint and occlusal forces (reaction forces on teeth), and $\mathbf{r}_m$, $\mathbf{r}_j$ and $\mathbf{r}_R$ are the moment arms for each muscular group, which were evaluated from the CT images by assuming the single force vector, muscle attachment and contact conditions.

A linear regression analysis was performed in this study by using Graph-Pad Prism 7 (GraphPad Software, Inc., CA, USA), to evaluate the coefficients of determination ($R^2$) and $p$ values. $R^2$ were calculated for the correlation between the clinical and computational data, in terms of the occlusal forces measured and calculated. The $p$ values were calculated to test against the null hypothesis that the overall slope of the fitted line is zero.

## 3. Results

### 3.1 Occlusal and medical imaging analysis

The clinical occlusal loads at time points M4, M16 and M28 are presented in Fig. 4. It can be found that the right mandibular C, one of the remaining teeth after surgery, carried significantly less occlusal loads in comparison with P1, P2 and M2 at Months 4 and 16. It therefore implies that P1, P2 and M2 were the primary teeth executing the occlusal function. In addition, an increase in the occlusal load was recorded from M4 to M28 for all the remaining teeth. It should be noted, nonetheless, that the standard deviation (SD) was significantly high for the measurements at M28, indicating substantial discrepancies of multiple measuring results *in vivo*.

### 3.2 Muscular force identification

$PCSAs$ were measured and are presented in Fig. 5a. Overall, declining trends were observed for most of the time and muscle groups from duration of BS to M16, except for LLP and RLP, in which a slight gain of capacity can be found from BS to M4 and from M16 to M28. In addition, no significant change was recorded from M16 to M28 for all the groups. The similar trend, due to linearity, occurred to the maximum capacity of masticatory muscles which were estimated accordingly and presented in Fig. 5b. All the five groups of muscles experienced evident declines in magnitude from M4 to M16 but remained almost unchanged thereafter (Fig. 5b). The maximum capacities of muscles Ma, MP, T, LLP and RLP were calculated to be 196.0 – 206.5 N, 145.4 – 151.3 N, 147.1 – 151.7 N, 181.7 – 191.2 N and 186.2 – 203.6 N, respectively. LLP and RLP, the only muscle pair of this resected mandible, presented comparably similar magnitudes throughout the entire observation period.

According to the identification results (Fig. 5b), the actual muscle forces presented different patterns in a time-dependent fashion. The magnitude of muscle Ma decreased slightly during the rehabilitation process; while muscle T increased slightly from M4 to M16, followed by almost no change towards M28. By comparison, muscle MP showed minimal change in magnitude, fluctuating around 116 N. Muscles LLP and RLP, on the other hand, varied greatly; specifically they decreased at M16 and then increased at M28. It was also evident that muscles MP and T exerted up to 80.3% of their corresponding maximum capacity during clenching, whereas muscles Ma, LLP and RLP used only 58.2%, 57.3% and 49.8% of their maximum capacity, respectively.

The linear regression analysis in Fig. 6a shows that the SKO technique yielded fairly high $R^2$ values, i.e. 0.92, 0.97 and 0.84, for time points M4, M16 and M28, respectively. The scatter generated by SKO was well fitted by the regression line. Conversely, $R^2$ values determined from the linear optimality criteria method were substantially lower and the corresponding data scattering was relatively poorly fitted by the regression line, indicating that use of conventional optimality criteria approach may not be able to generate accurate occlusal loads, at least for the case involving major oral intervention such as jaw reconstruction across different stages of rehabilitation (Fig. 6a). As a result, the displacement contours generated by the linear optimality methods are visibly deviated from those obtained from the SKO method (Fig. 6b).

## 4. Discussion

The sequential Kriging optimization (SKO) based inverse identification technique as proposed in this study quantified the muscle force components (magnitudes and directions) during the maximum voluntary clenching at different time points, by virtue of the *in vivo* measurements of occlusal loads. In contrast, the conventional methods assume that the input, output (i.e. muscle force, reaction force and joint force in this case) or their combination tends to be minimum overall during muscle co-activation, physiologically (Chou et al., 2015; Nubar and Contini, 1961; Osborn and Baragar, 1985; Pedotti et al., 1978; Schindler et al., 2007). Our comparative study showed that SKO could detail the resultant muscular force magnitudes and directions with fairly high $R^2$ values against the occlusal measurements *in vivo*, ranging from 0.84 to 0.97, attesting to its effectiveness and accuracy. Conversely, the optimal control theory resulted in the occlusal loads significantly diverging from the clinical measurements in the course of rehabilitation (Fig. 6a).

The deduction herein is that while the neuro-musculo-skeletal system still tends to reduce, if not to minimize the consumption of energy, or the potential detriment to tissues, it is unlikely to provide an absolute optimal behavior which may define a limit that our body can hardly achieve. In other words, it can be sufficiently good rather than optimally best (Loeb, 2012). The central nervous system (CNS) may be as complex as computing power but would address the masticatory coordination in a way different from the single-objective optimization that seeks ideal solution based upon a large number of statistically randomized samples and corresponding outputs (De Rugy et al., 2012). On the other hand, the CNS has no capability of foreseeing the results but referring to the feedbacks from the relevant biochemical events accumulatively (Kistemaker et al., 2010). Such an inherent distinction between human and computer may to a certain extent restrict the favourability and effectiveness of using traditional optimality criterion approaches for determining the muscular activation and functionality, at least for such a jaw reconstruction case.

Despite the ongoing applications of minimization strategy in human locomotion and neuroscience studies, the forgoing conclusions indicated that the preferable muscular patterns (e.g. during gaiting, arm or wrist movements and running) may not be always consistent with or solely dominated by a single-objective optimization for minimizing metabolic consumption (De Rugy et al., 2012; Hunter et al., 2010; Kistemaker et al., 2010; Miller et al., 2011; Morgan et al., 1994). It may be irrational to use a single optimality criterion for determining entire masticatory muscle activity during mastication. Further, it is speculated that as the mastication has a relatively narrower range of motion, compared with the other types of locomotion such as gaiting and running, the CNS may have relatively smaller ranges of control to regulate the muscular activity beneficially, i.e. reduce the energy consumption or harm.

Due to its substantial role in stomatognathic performance, masticatory functionality has been directly or indirectly measured using a range of different methods to date, including EMG (Van Ruijven and Weijs, 1990), CT-based imaging analysis (Katsumata et al., 2004), gnathodynamometer (Marunick et al., 1992a), colour-changing gum (Shibuya et al., 2013), gummy jelly (Shiga et al., 2012), questionnaires (Sato et al., 1989) and the above-mentioned optimality criteria (Schindler et al., 2007) techniques. None of these methods alone can produce the proper quantification of muscle force in both magnitude and direction. The inverse identification approach proposed in this study allows addressing this issue with its advantage of matching the clinical data collected over a 28-month rehabilitation course.

As shown in Fig. 5, the results indicate that the maximum capacity of muscular contraction could slightly decrease at the early stage of rehabilitation, caused by the reduction of $PCSA$. This finding was consistent with that by Dicker *et al*. (Dicker et al., 2007), in which the shrinkage of $PCSA$ was found for muscles Ma and MP at the 18 months after the bilateral sagittal split osteotomies. In literature, Katsumata *et al*. (Katsumata et al., 2004) also reported the reduction in $PCSA$ of Ma following mandibular setback osteotomy. This could be attributable to the muscular atrophy as a consequence of the dissection of bony and muscular tissues by neglecting re-joining with the surrounding tissues for recovering substantial muscle force over time, hypothetically causing the regional interference with the blood supply (Conley and Lindstedt, 2002; López-Arcas et al., 2010; Sieg et al., 2002). Nonetheless, it is found that $PCSA$ stopped decreasing after M16 in this specific case, indicating a stabilizing functional condition of the muscles in the resected regions undergoing certain rehabilitation.

The activation ratio and actual muscle force generated here, however, witnessed dissimilar patterns with irregular fluctuations (Fig. 5b). The activation rates of muscles Ma and T with complete dentitions during maximum voluntary clenching were reported to be laid in between 70.3% and 77.7% (Hattori et al., 2003), which is higher than that of Ma (53.0 - 58.2%) and on par with that of T (71.7 - 80.0%), as calculated in this study. This implies that the hesitation of the patient to bite, especially using the resected side, has a major effect on Ma, reducing its activation ratio by supposedly 20% from the normal (Marunick et al., 1992b). Furthermore, due to the lack of consideration of different biting strategies, the present results might only be able to explain a particular situation (i.e. clenching) (Ogawa et al., 2006).

Furthermore, inconsiderable consecutive decreases in force magnitude of muscle Ma were recorded throughout the rehabilitation follow-up, echoing the outcomes of the study by Nakata *et* *al*. (Nakata et al., 2007) in which the Ma activity was measured to decrease slightly for 31 months after mandibular prognathism. In comparison, MP presented no significant change from M4 to M28 in the maximum muscular capacity, activation ratio and actual resultant muscle force (Fig. 5). Different patterns were observed with LLP and RLP, in which the activation ratios and actual muscle forces decreased from M4 to M16, but subsequently increased and surpassed the M4 values at M28. The loss of some major masticatory muscles in the resection side (right) led to non-physiological conditions, which can considerably alter the normal muscle activities for re-stabilizing the reconstructed mandible, implying that the higher activation rates of MP and T might thus be related to the stabilization of mandibular position. The reason why the calculated muscle forces were high for the LLP and RLP, can be due to the lack of suprahyoid muscles, such as the mylohyoid muscles, which contribute on stabilization of the mandible during biting. Another possible reason is that the vertical direction of the occlusal force was applied in FEA. The force direction *in vivo* can actually tilt ipsilaterally (Kawata 2007). Considering the jaw biomechanics, the lateral force vector of LPTs may be needed to ensure force vertically in the model.

One of the limitations in this study is the sample size for its patient specific nature. First, only one patient, who underwent a major mandibular resection/reconstruction, has been followed up over a rehabilitation course of 28 months. While it is not advocated, given the uniqueness of the case, the findings of this study could still shed lights on the determination of a more realistic masticatory pattern for a large population, including those with normal or nearly normal masticatory functionality. A future study should therefore recruit more patients with demographic and clinical variances over a longer course of rehabilitation. Second, the present study has focused on the static equilibrium when occlusion occurred, whereby its dynamic characteristics were not investigated, which could have caused the results to deviate from reality to a certain extent. Third, the high standard deviation of occlusal measurements at M28 may render that the evaluation of muscular activity at this time point could be less accurate, while it also indicates the instability of masticatory patterns not long after the introduction of the dental crown.

Overall, this study developed a new framework by correlating the clinical measurements *in vivo* with numerical modeling *in silico* at different time points for quantifying the magnitudes and directions of oral muscle forces. An effective identification procedure was established here to determine patient-specific muscular activities inversely in the course of 28-month rehabilitation. This method has proven to significantly improve the accuracy and reliability of conventional gradient-based optimization techniques which minimize overall energy consumption. This study and SKO approach exhibits considerable potentials for the further development of digitalizing major intervention of maxillofacial surgery.

**Acknowledgements**

We are grateful to Dr. Shigeto Koyama, Dr. Atsushi Takeda and Dr. Naoko Sato for recruiting and caring for the patient. This work was supported by Australian Research Council (ARC) through the Discovery Scheme (DP160104602). The first and second authors are the recipients of Australian Postgraduate Award (APA) at The University of Sydney.

**Conflict of interest**

Authors have no conflict of interest concerning the present manuscript.

## Figure captions

**Abstract.** This study developed a new framework by correlating the clinical measurements *in vivo* with numerical modeling *in silico* at different time points for quantifying the magnitudes and directions of oral muscle forces.

**Fig. 1.** (*a*) Occlusal force measurement using pressure-indicating film. (*b*) Silicone impression as bite records from maxilla view, and (*c*) from mandible view.

**Fig. 2.** Estimation of muscle physiological cross-sectional areas (PCSA). (*a*) Reference planes for measuring PCSA of Ma (red line), MP (red line) and T (purple line) and (*b*) LP (green line). (*c*) Examples of muscle PCSA of Ma and MP, (*d*) T and (*e*) LPs.

**Fig. 3.** FE model with illustration of loading and boundary conditions (at M16).

**Fig. 4** Clinically measured occlusal loading changes with standard deviations, at 4(M4), 16 (M16) and 28 (M28) months after mandibular reconstruction

**Fig. 5.** (*a*) $PCSA$ changes before and after surgery. (*b*) CT-derived maximum muscle capacities and the identified muscle force magnitudes at time points M4, M16 and M28; AR are also shown on top of each bar.

**Fig. 6.** (*a*) Regression analysis between occlusal forces obtained from the proposed identification procedure and experimental measurements; (*b*) Comparison of displacement magnitude contours at M4, M16 and M28, using different optimization techniques. Vectors of the displacements at the specific points of interests were illustrated.

## References


Al-Ahmari, A., Nasr, E.A., Moiduddin, K., Anwar, S., Kindi, M.A., Kamrani, A., 2015. A comparative study on the customized design of mandibular reconstruction plates using finite element method. Advances in Mechanical Engineering 7, 1687814015593890.

Chen, J., Ahmad, R., Suenaga, H., Li, W., Sasaki, K., Swain, M., Li, Q., 2015. Shape optimization for additive manufacturing of removable partial dentures-A new paradigm for prosthetic CAD/CAM. PloS one 10, e0132552.

Chou, H.-Y., Satpute, D., Müftü, A., Mukundan, S., Müftü, S., 2015. Influence of mastication and edentulism on mandibular bone density. Computer methods in biomechanics and biomedical engineering 18, 269-281.

Conley, K.E., Lindstedt, S.L., 2002. Energy-saving mechanisms in muscle: the minimization strategy. Journal of experimental biology 205, 2175-2181.

Cruz, M., Wassall, T., Toledo, E.M., da Silva Barra, L.P., de Castro Lemonge, A.C., 2003. Three-dimensional finite element stress analysis of a cuneiform-geometry implant. International Journal of Oral & Maxillofacial Implants 18.

De Rugy, A., Loeb, G.E., Carroll, T.J., 2012. Muscle coordination is habitual rather than optimal. Journal of Neuroscience 32, 7384-7391.

Dicker, G., Van Spronsen, P., Van Schijndel, R., van Ginkel, F., Manoliu, R., Boom, H., Tuinzing, D.B., 2007. Adaptation of jaw closing muscles after surgical mandibular advancement procedures in different vertical craniofacial types: a magnetic resonance imaging study. Oral Surgery, Oral Medicine, Oral Pathology, Oral Radiology and Endodontics 103, 475-482.

Endo, N., 1972. Studies on masticatory functions in patients with surgical mandibular reconstruction. Oral Surgery, Oral Medicine, Oral Pathology and Oral Radiology 34, 390-407.

Fang, J., Sun, G., Qiu, N., Kim, N.H., Li, Q., 2017. On design optimization for structural crashworthiness and its state of the art. Structural and Multidisciplinary Optimization 55, 1091-1119.

Faulkner, M., Hatcher, D., Hay, A., 1987. A three-dimensional investigation of temporomandibular joint loading. Journal of biomechanics 20, 997-1002.

Field, C., Li, Q., Li, W., Thompson, M., Swain, M., 2010. Prediction of mandibular bone remodelling induced by fixed partial dentures. Journal of biomechanics 43, 1771-1779.

Fukunaga, T., Kubo, K., Kawakami, Y., Fukashiro, S., Kanehisa, H., Maganaris, C.N., 2001. In vivo behaviour of human muscle tendon during walking. Proceedings of the Royal Society of London B: Biological Sciences 268, 229-233.

Gonda, T., Yasuda, D., Ikebe, K., Maeda, Y., 2014. Biomechanical factors associated with mandibular cantilevers: analysis with three-dimensional finite element models. International Journal of Oral & Maxillofacial Implants 29.

Hattori, Y., Satoh, C., Seki, S., Watanabe, Y., Ogino, Y., Watanabe, M., 2003. Occlusal and TMJ loads in subjects with experimentally shortened dental arches. Journal of dental research 82, 532-536.

Hidaka, O., Iwasaki, M., Saito, M., Morimoto, T., 1999. Influence of clenching intensity on bite force balance, occlusal contact area, and average bite pressure. Journal of Dental Research 78, 1336-1344.

Hunter, L., Hendrix, E., Dean, J., 2010. The cost of walking downhill: is the preferred gait energetically optimal? Journal of biomechanics 43, 1910-1915.

Katsumata, A., Fujishita, M., Ariji, Y., Ariji, E., Langlais, R.P., 2004. 3D CT evaluation of masseter muscle morphology after setback osteotomy for mandibular prognathism. Oral Surgery, Oral Medicine, Oral Pathology and Oral Radiology 98, 461-470.

Kistemaker, D.A., Wong, J.D., Gribble, P.L., 2010. The Central Nervous System Does Not Minimize Energy Cost in Arm Movements. Journal of Neurophysiology 104, 2985-2994.

Korioth, T.W., Romilly, D.P., Hannam, A.G., 1992. Three - dimensional finite element stress analysis of the dentate human mandible. American Journal of Physical Anthropology 88, 69-96.

Liao, Z., Chen, J., Li, W., Darendeliler, M.A., Swain, M., Li, Q., 2016. Biomechanical investigation into the role of the periodontal ligament in optimising orthodontic force: A finite element case study. Archives of oral biology 66, 98-107.

Liao, Z., Chen, J., Zhang, Z., Li, W., Swain, M., Li, Q., 2015. Computational modeling of dynamic behaviors of human teeth. Journal of biomechanics 48, 4214-4220.

Liao, Z., Yoda, N., Chen, J., Zheng, K., Sasaki, K., Swain, M.V., Li, Q., 2017. Simulation of multi-stage nonlinear bone remodeling induced by fixed partial dentures of different configurations: a comparative clinical and numerical study. Biomech. Model. Mechanobiol. 16, 411-423.

Loeb, G.E., 2012. Optimal isn’t good enough. Biological cybernetics 106, 757-765.

López-Arcas, J.M., Arias, J., Del Castillo, J.L., Burgueño, M., Navarro, I., Morán, M.J., Chamorro, M., Martorell, V., 2010. The fibula osteomyocutaneous flap for mandible reconstruction: a 15-year experience. Journal of Oral and Maxillofacial Surgery 68, 2377-2384.

Marunick, M., Mathes, B.E., Klein, B.B., Seyedsadr, M., 1992a. Occlusal force after partial mandibular resection. Journal of Prosthetic Dentistry 67, 835-838.

Marunick, M., Mathes, B.E., Klein, B.B., Seyedsadr, M., 1992b. Occlusal force after partial mandibular resection. The Journal of prosthetic dentistry 67, 835-838.

Miller, R.H., Umberger, B.R., Hamill, J., Caldwell, G.E., 2011. Evaluation of the minimum energy hypothesis and other potential optimality criteria for human running. Proceedings of the Royal Society of London B: Biological Sciences, rspb20112015.

Morgan, D., Martin, P., Craib, M., Caruso, C., Clifton, R., Hopewell, R., 1994. Effect of step length optimization on the aerobic demand of running. Journal of Applied Physiology 77, 245-251.

Nakata, Y., Ueda, H.M., Kato, M., Tabe, H., Shikata-Wakisaka, N., Matsumoto, E., Koh, M., Tanaka, E., Tanne, K., 2007. Changes in stomatognathic function induced by orthognathic surgery in patients with mandibular prognathism. Journal of oral and maxillofacial surgery 65, 444-451.

Namaki, S., Matsumoto, M., Ohba, H., Tanaka, H., Koshikawa, N., Shinohara, M., 2004. Masticatory efficiency before and after surgery in oral cancer patients: comparative study of glossectomy, marginal mandibulectomy and segmental mandibulectomy. Journal of oral science 46, 113-117.

Nubar, Y., Contini, R., 1961. A minimal principle in biomechanics. The bulletin of mathematical biophysics 23, 377-391.

Ogawa, T., Kawata, T., Tsuboi, A., Hattori, Y., Watanabe, M., Sasaki, K., 2006. Functional properties and regional differences of human masseter motor units related to three‐dimensional bite force. Journal of oral rehabilitation 33, 729-740.

Osborn, J., Baragar, F., 1985. Predicted pattern of human muscle activity during clenching derived from a computer assisted model: symmetric vertical bite forces. Journal of biomechanics 18, 599-612.

Peck, C., Langenbach, G., Hannam, A., 2000. Dynamic simulation of muscle and articular properties during human wide jaw opening. Archives of Oral Biology 45, 963-982.

Pedotti, A., Krishnan, V., Stark, L., 1978. Optimization of muscle-force sequencing in human locomotion. Mathematical Biosciences 38, 57-76.

Pepato, A.O., Palinkas, M., Regalo, S.C.H., Ribeiro, M.C., Souza, T.A.S., Siéssere, S., de Sousa, L.G., Sverzut, C.E., Trivellato, A.E., 2013. Analysis of masticatory efficiency by electromyographic activity of masticatory muscles after surgical treatment of zygomatic-orbital complex fractures. international journal of stomatology & occlusion medicine 6, 85-90.

Pruim, G., De Jongh, H., Ten Bosch, J., 1980. Forces acting on the mandible during bilateral static bite at different bite force levels. Journal of biomechanics 13, 755-763.

RENAUD, M., MERCIER, P., VINET, A., 1984. Mastication after surgical reconstruction of the mandibular residual ridge. Journal of oral rehabilitation 11, 79-84.

Rues, S., Lenz, J., Türp, J.C., Schweizerhof, K., Schindler, H.J., 2008. Forces and motor control mechanisms during biting in a realistically balanced experimental occlusion. Archives of oral biology 53, 1119-1128.

Sato, Y., Minagi, S., Akagawa, Y., Nagasawa, T., 1989. An evaluation of chewing function of complete denture wearers. The Journal of prosthetic dentistry 62, 50-53.

Schindler, H., Rues, S., Türp, J., Schweizerhof, K., Lenz, J., 2007. Jaw clenching: muscle and joint forces, optimization strategies. Journal of dental research 86, 843-847.

Seireg, A., Arvikar, R., 1973. A mathematical model for evaluation of forces in lower extremeties of the musculo-skeletal system. Journal of biomechanics 6, 313-322.

Shibuya, Y., Ishida, S., Hasegawa, T., Kobayashi, M., Nibu, K., Komori, T., 2013. Evaluating the masticatory function after mandibulectomy with colour‐changing chewing gum. Journal of oral rehabilitation 40, 484-490.

Shiga, H., Kobayashi, Y., Katsuyama, H., Yokoyama, M., Arakawa, I., 2012. Gender difference in masticatory performance in dentate adults. Journal of prosthodontic research 56, 166-169.

Sieg, P., Zieron, J., Bierwolf, S., Hakim, S., 2002. Defect-related variations in mandibular reconstruction using fibula grafts.: A review of 96 cases. British Journal of Oral and Maxillofacial Surgery 40, 322-329.

Van Ruijven, L., Weijs, W., 1990. A new model for calculating muscle forces from electromyograms. European journal of applied physiology and occupational physiology 61, 479-485.

Weijs, W., Hillen, B., 1984. Relationships between masticatory muscle cross-section and skull shape. Journal of Dental Research 63, 1154-1157.

Weijs, W., Hillen, B., 1985. Physiological cross-section of the human jaw muscles. Cells Tissues Organs 121, 31-35.

Fig.1

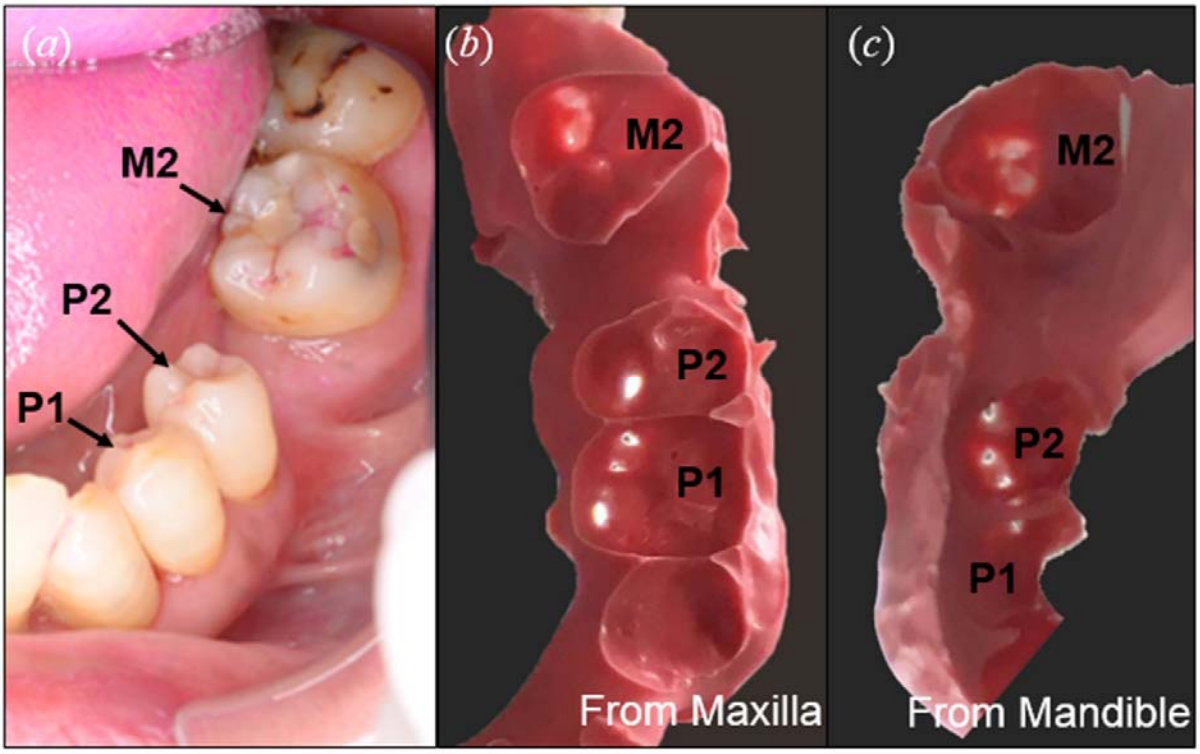

Fig. 2

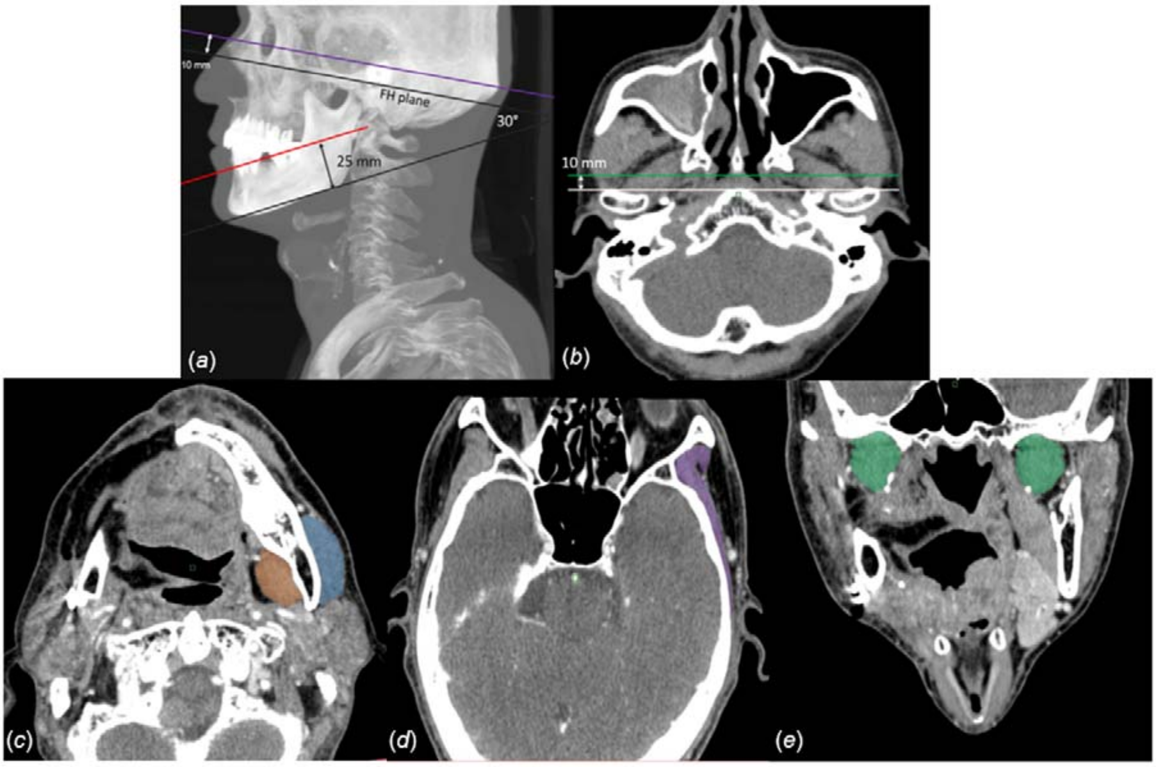

Fig. 3

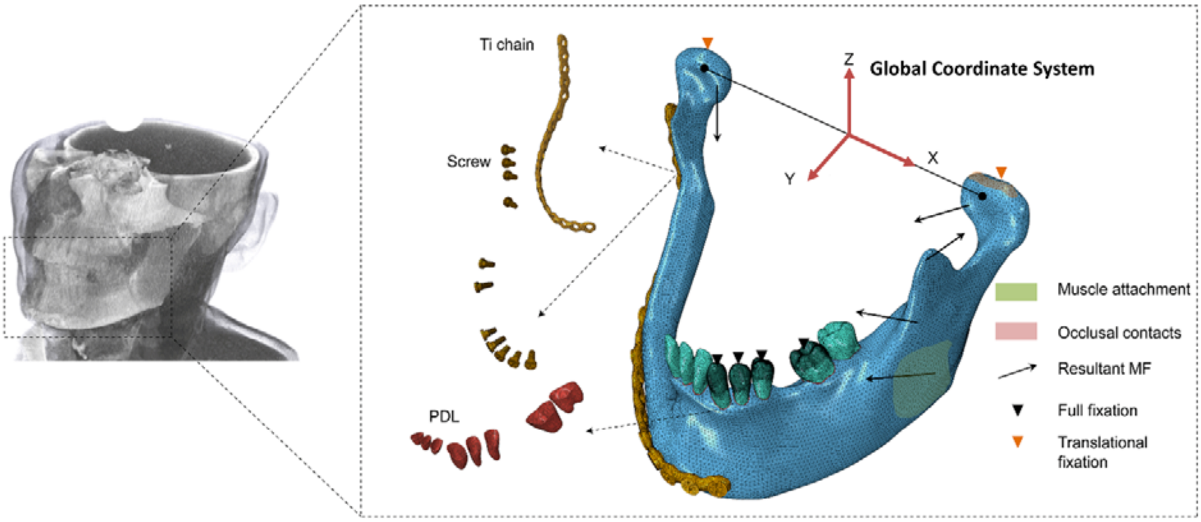
Ti chain
Screw
PDL
Global Coordinate System
Z
Y
X
Muscle attachment
Occlusal contacts
Resultant MF
Full fixation
Translational fixation

Fig. 4

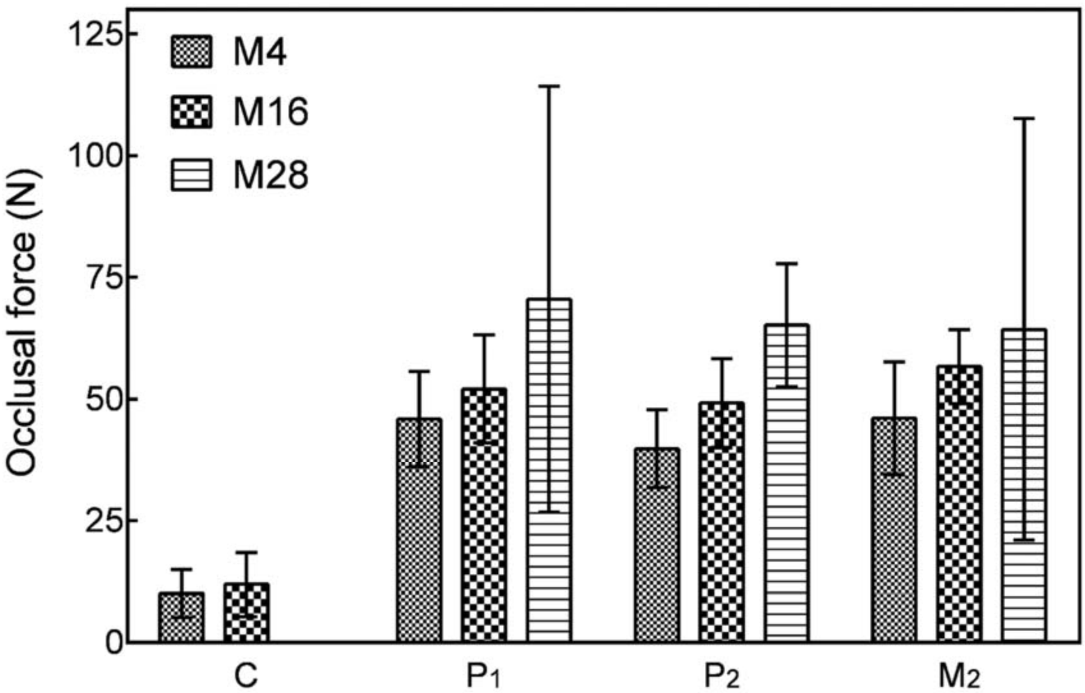

Fig. 5

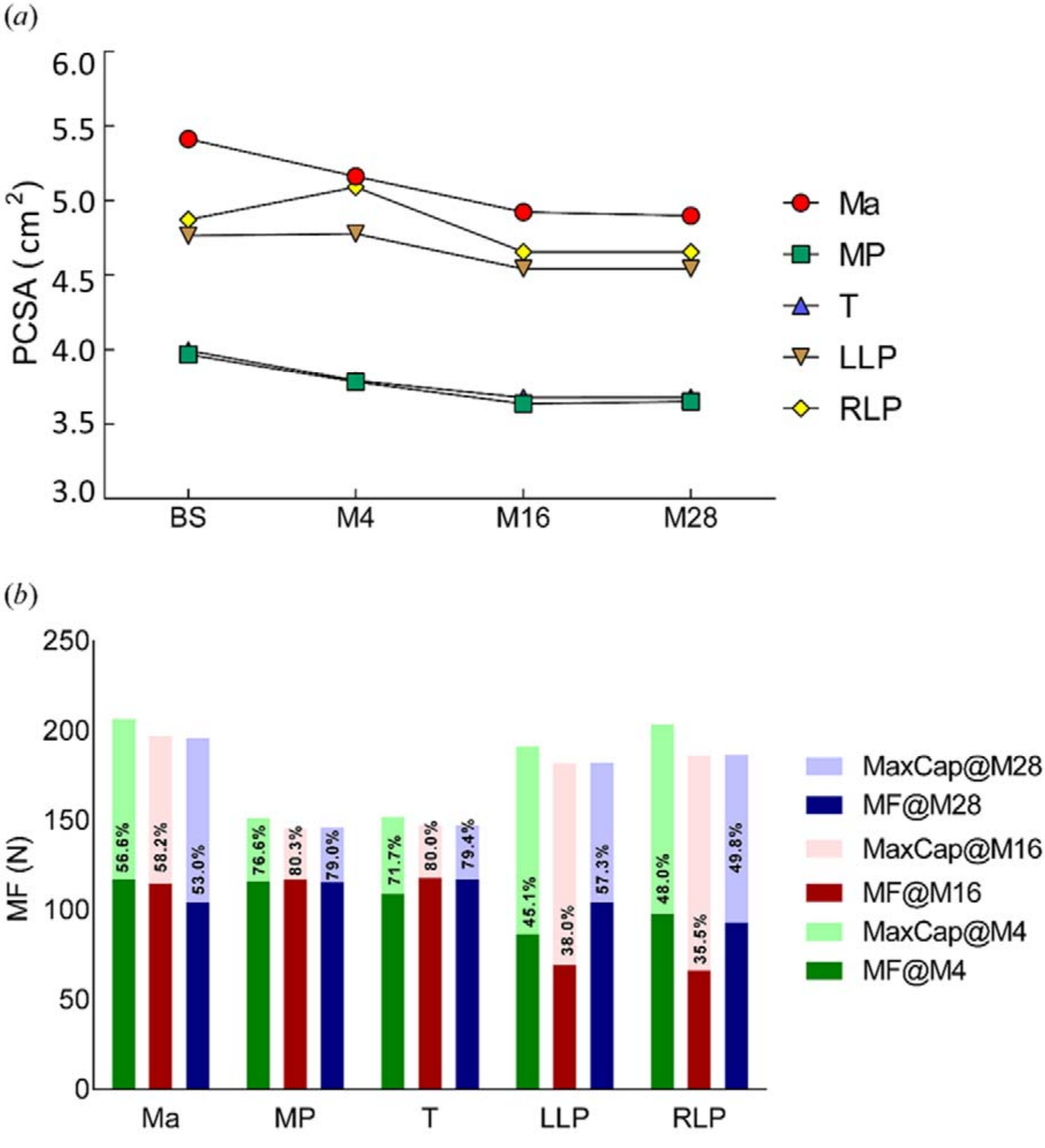
(a)
PCSA ( cm 2)
6.0
5.5
5.0
4.5
4.0
3.5
3.0
BS
M4
M16
M28
Ma
MP
T
LLP
RLP
(b)
MF (N)
250
200
150
100
50
0
Ma
MP
T
LLP
RLP
56.6%
58.2%
53.0%
76.6%
80.3%
79.0%
71.7%
80.0%
79.4%
45.1%
38.0%
57.3%
48.0%
35.5%
49.8%
MaxCap@M28
MF@M28
MaxCap@M16
MF@M16
MaxCap@M4
MF@M4

Fig. 6

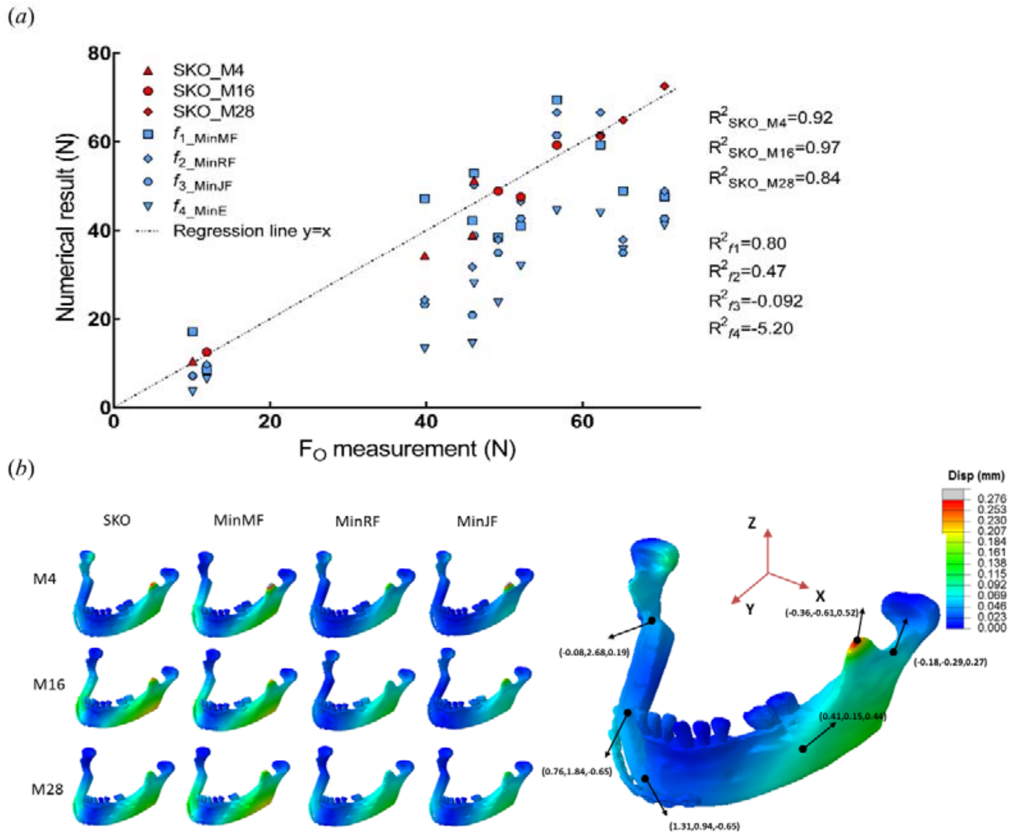
(a)
SKO_M4
SKO_M16
SKO_M28
f1_MinMF
f2_MinRF
f3_MinJF
f4_MinE
Regression line y=x
Numerical result (N)
FO measurement (N)
R2SKO_M4=0.92
R2SKO_M16=0.97
R2SKO_M28=0.84
R2f1=0.80
R2f2=0.47
R2f3=-0.092
R2f4=-5.20
(b)
SKO
MinMF
MinRF
MinJF
M4
M16
M28
Disp (mm)
Z
X
Y